Supplementary Information: A possible infinite number of components in a single crystalline phase: on the isomorphism of brivaracetam – guest molecules

Nicolas Couvrat[†], Morgane Sanselme[†], Yohann Cartigny[†], Frederic De Smet[‡], Sandrine Rome[‡], Luc Aerts[‡], Luc Quéré[‡], Johan Wouters[#], Gérard Coquerel[†]**

[†] Normandie Univ, UNIROUEN-Normandie, EA3233, Laboratoire Science et Méthodes Séparatives, 76821 Mont Saint Aignan, France.

[‡] UCB Pharma S.A., 1420 Braine l'Alleud, Belgium.

[#] Université de Namur Unité de chimie physique, théorique et structurale 5000 Namur, Belgium.

I. Experimental Section

Brivacetam (IUPAC name: (2S)-2-[(4R)-2-oxo-4-propyl-pyrrolidin-1-yl] butanamide), $C_{11}H_{20}N_2O_2$, was directly supplied by UCB Pharma (99% purity) and was used with no further purification. Every chemical used as guest molecules was provided from either Acros Organics or Alfa Aesar. For pure components, a given purity of at least 98% was selected.

Preparation of Phase(s) 2 was performed by two different methods:
i) for liquid guests, a suspension of BRV in the guest (50/50 % w/w) was prepared at room temperature and maintained under stirring during 24 hours. The crystallization of Phase 2 was generally indicated by a massive crystallization throughout the solution. Phase 2 crystalline powders was then recovered by filtration and their characterization was achieved by X-Ray Powder Diffraction (XRPD) and Dynamic Scanning Calorimetry analyses (DSC).
ii) for solid guests, a co-grinding was performed on a 50/50 w/w mixture between BRV and the guest using a vibratory mill Retsch MM400. Milling duration was fixed at 30 minutes and milling frequency at 30 Hz. After milling, the resulting solid was directly recovered and analyzed by XRPD and DSC analyses in order to confirm the presence of Phase 2.

Suitable single crystals of Phase 1 were obtained by slow solvent evaporation of a saturated solution in acetone at ambient temperature.
Suitable single crystals of Phase 2 with Isopropyl acetate were obtained by slow solvent evaporation of a saturated solution at ambient temperature.

Suitable crystals of Phase 2 with PEG100 stearate were obtained by co-melting both components at 83°C and cooling down to 50°C.

XRPD measurements were carried out on a Bruker D5000 Matic Discover with a Bragg Brentano geometry, in -theta/-theta reflection mode. The instrument is equipped with a copper anticathode (40 kV, 40 mA) and a scintillation counter detector. The diffraction patterns were collected by steps of 0.04° (in 2-theta) over the angular range 3–30°, with a counting time of 4s per step.

DSC analyses were carried out with a DSC device 204 F1 Phoenix (Netzsch) equipped with an Intracooler (-40°C) and a carrousel. Mass samples of circa 5mg were weighted in 25 µL aluminium pans with pierced lids. Helium was used as purging and drying gas and the heating rate was fixed at 5°C/min.

Hot Stage-microscopy: Microscopy observations with controlled temperature, samples were loaded into a quartz cell with a cylindrical geometry (d=13 mm, h=1.3 mm) and sampled in a THMS 600 temperature stage setup (Linkam) to allow for accurate control of the sample temperature (± 0.1 °C). The setup is coupled with a Nikon Eclipse LV100 microscope (maximum magnification: x1000) connected to a computer for image captures by using a CCD camera.
DVS: Solvent vapor sorption and desorption are carried out with an accurate partial solvent pressure and temperature controlled microbalance system (DVS Advantage plus type, Surface Measurement System, UK). The partial vapor pressure is controlled by continuous gas flow containing pure nitrogen and solvent vapor in adequate proportions. The temperature and the partial vapor pressure are directly measured with a precision of +/- 0,5°C and +/- 0,5% respectively. Mass variations are recorded continuously with a precision of 0.1 µg.
Remark: the partial vapor pressure is expressed in %, it corresponds to the ratio between partial vapor pressure over the saturated vapor pressure at a fixed temperature ($=P_{solvent}/P_{sat}$). The mass variation and the partial pressure are measured automatically. The increment in $P_{solvent}/P_{sat}$ is driven by a mass evolution criterion (dm/dt<5x10-4%.min-1 during 10 minutes). The maximum stabilization time was adjusted to 2000 minutes.

II. Crystallographic studies

The crystal structures were determined from single crystal diffraction on either a SMART APEX diffractometer (with MoKα1 radiation, λ: 0.71073 A) or a Gemini Ultra diffractometer (using CuKα1 radiation, λ : 1.54184 A). The structures were solved by direct methods (SHEL-XS [1]). Anisotropic displacement parameters were refined for all non-hydrogen atoms using SHEL-XL [2] available with the WinGX [3] package. All hydrogen atoms were included in the models in calculated positions and were refined as contained to bonding atoms.

[1] include in WinGX suite: SIR 92: A. Altomare, G. Cascarano, & A. Gualardi (1993) J. Appl. Cryst. 26, 343-350; SHELXS-97: Sheldrick, G. M., (1990) Acta cryst, A46, 467.
[2] include in WinGX suite: SHELXL-97 – a program for crystal structure refinement, G. M. Sheldrick, University of Goettingen, Germany, 1997, release 97-2.
[3] WinGX: Version 1.70.01: An integrated system of Windows Programs for the solution, refinement and analysis of Single Crystal X-Ray Diffraction Data, By Louis J. Farrugia, Dept. of chemistry, University of Glasgow. L. J. Farrugia (1999) J. Appl. Cryst. 32, 837-838.

III. Detailed views of the crystal structures

II.1. BRV Phase 1

Figure S1 displays a projection along (b) axis of several unit cells of Phase 1

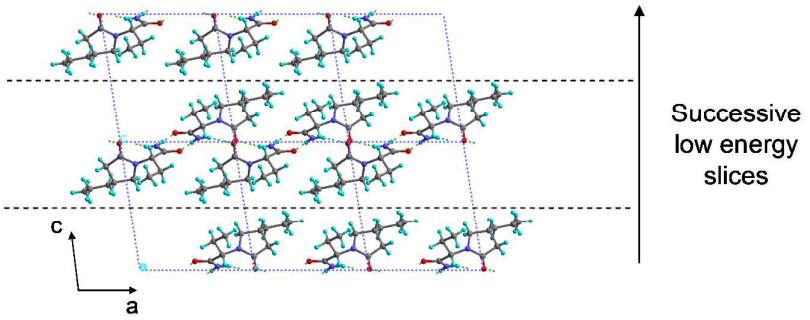

Figure S1: Projection along b axis of neighboring lattices of BRV Phase 1

Each BRV molecule is linked to four other molecules via two hydrogen bonds (see Table S1).

Table S1: Table of Hydrogen bonds for BRV phase 1

D-H...A	d(H...A)	d(D...A)	Angles between D-H..A
N(1)-H(1A)...O(1)#1	2.11Å	2.961(2)Å	172.5°
N(1)-H(1B)...O(2)#2	2.11Å	2.929(2)Å	158.5°

Symmetry transformation used to generate equivalent atom

#1 -x+2,y+1/2,-z+2 ; #2 -x+1,y+1/2,-z+2

These hydrogen bonds lead to the formation of low energy slices, which corresponds to (001) orientations. These layers are linked by Van der Waals interactions (figure S1). The calculated crystal morphology of Phase 1, linked to the single crystal shape obtained in acetone is presented in figure S2.

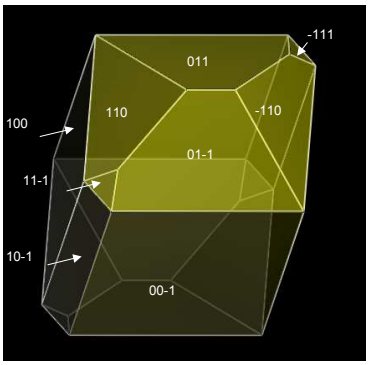

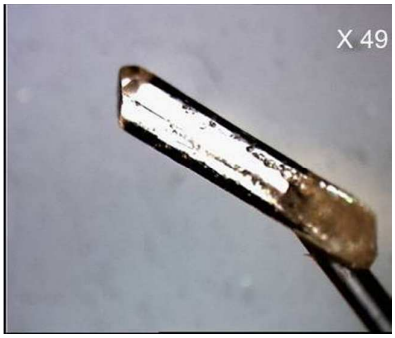

a) b)

Figure S2: Crystal morphologies of BRV Phase 1 determined by BFDH method (a) and single crystal of phase 1 obtained in acetone (b). BFDH morphology was determined by using Material Studio (Accelrys inc.)

II.1. BRV Phase 2

Figure S3 displays a projection along c axis of BRV phase 2.

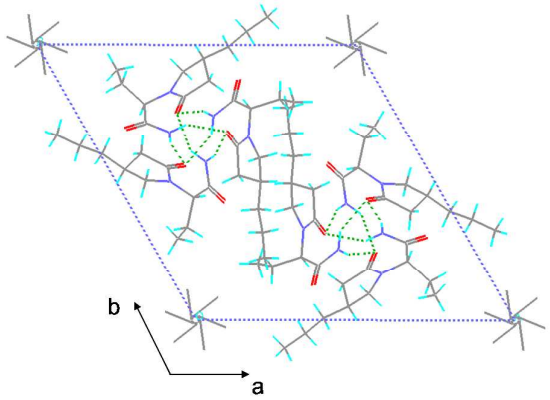

Figure S3: Projection along c axis of BRV phase 2 (crystallized in isopropyl acetate)

In this structure, the oxygen atom of the amide moiety does not take part to the H bond network. Only the oxygen atom of the heterocyclic carbonyl acts as H-bond acceptors.

The nitrogen atom of amide group remains a H-bond donor, and forms two bonds with its neighbouring atoms (see table S2).

Table S2: Table of Hydrogen bonds for BRV phase 2

D-H...A	d(H...A)	d(D...A)	Angles between (D-H..A)
N(2)-HN21...O(1)#1	2.24(6) Å	3.077(6) Å	162(4)
N(2)-HN22...O(1)#2	2.06(5) Å	2.929(5) Å	146(4)

Symmetry transformation used to generate equivalent atom:

#1 -y+1,x-y,z-2/3 ; #2 -x+y+1,-x+1,z-1/3

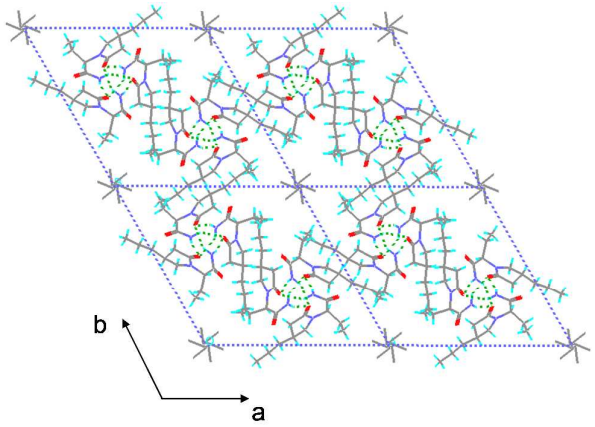

Figure S4: Structural representation along c axis of four lattices of BRV Phase 2 (crystallized in isopropyl acetate)

The representation of figure S4**Figure** shows a channel whose diameter is circa: 8.2 Å. Residual electronic density was detected inside this channel. On figure S5, molecules are represented in spacefill, which allows a better perception of the free space inside Phase 2 channels.

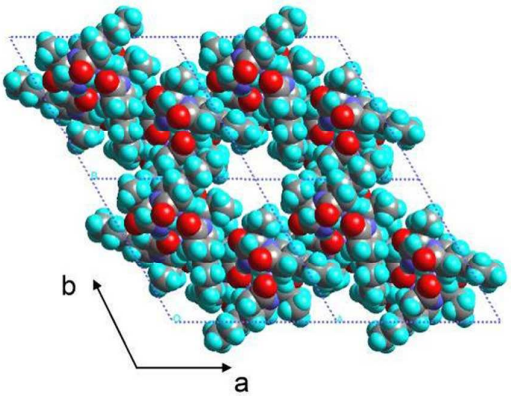

Figure S5: Spacefill representation of 4 BRV Phase 2 unit cells

Phase 2 crystallizes with a needle shape along the 6-fold axis (figure S6), which allows a clear identification by optical microscopy.

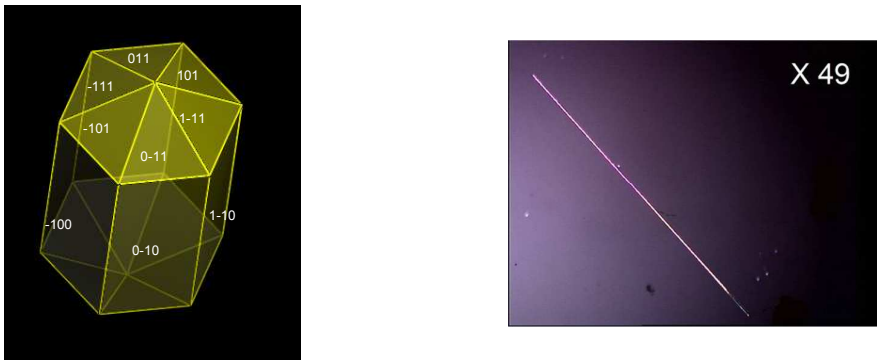

a) b)

Figure S6: Crystal morphologies of BRV phase 2 determined by BFDH method (a) and single crystal of BRV phase 2 obtained in isopropyl acetate. (b) BFDH morphology was determined by using Material Studio (Accelrys inc.)

IV. Binary Phase diagram with n-dodecane

Binary phase diagrams between BRV and n-heptane in the one hand and n-dodecane in the other hand were determined by combination of X-Ray Powder Diffraction (XRPD), Dynamic Scanning Calorimetry (DSC), Hot-Stage microscopy (HSM) and Dynamic Vapor Sorption (DVS) analyses.

The isobaric phase diagram (P= 1atm) BRV/n-heptane determined is presented in figure 3 in the manuscript. The isobaric phase diagram (P= 1atm) BRV/n-dodecane is presented in figure S7. The stoichiometry of Phase 2 is deduced from DVS analyses, but putative solid solution is proposed as a function of the temperature (doted lines).

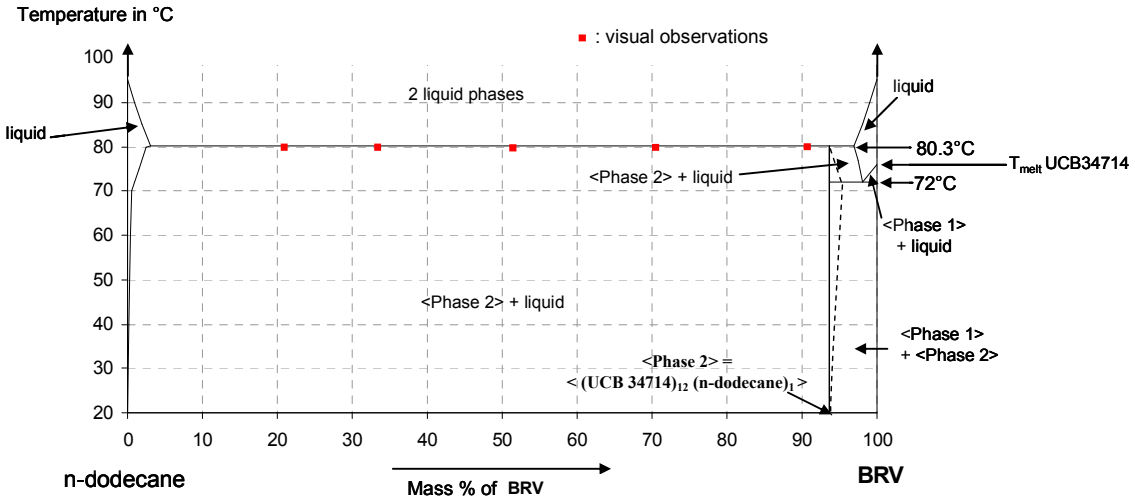

Figure S7: Isobaric (P= 1atm) binary diagram of the system BRV/ n-dodecane

V. Crystallization of Phase 2 by co-melting

Phase 2 can be crystallized with linear paraffins when the initial mixture (BRV + parrafin) is placed at a temperature above both starting components melting points (T_m). Figure S8 displays an example of co-melting experiment with n-dotriacontane.

a) b)

Figure S8. Co-melting pictures illustrating the BRV phase 2 crystallization with n-dotriacontane at the liquids interface: a) starting situation at 25°C, b) after 12 hours at 80°C (ventilated oven). Note that T_m~Phase 1= 76°C and T_m $C_{32}H_{66}$=70°C.

VI. List of co-formers with Phase 2

Table S3 displays the list of the co-formers which were proven (so far) to initiate Phase 2 formation with BRV. This list is not exhaustive and could be extended in particular for linear alkanes which should always form Phase 2 with BRV whatever their length or odd-even character.

Table S3: List of tested and validated co-formers for BRV Phase 2

Linear alkanes	**Alcohols**
n-pentane	1-undecanol
n-hexane	1-octanol
n-heptane	
n-octane	**Ethers**
n-nonane	tert-butylmethylether
n-decane	cyclopentyl methyl ether
n-undecane	diethyl ether
n-dodecane	isopropyl ether
n-hexadecane	
n-octadecane	**Fatty acids and derivatives**
n-nonadecane	stearic acid
n-eicosane	linoleic acid
n-heneicosane	oleic acid
n-tetracosane	stearic acid methyl ester
n-dotriacontane	n-dodecanoic acid (i.e. Lauric acid)
	n-tetradecanoic acid (i.e. Myristic
n-tetracontane	acid)
n-pentacontane	n-docosanoic acid (i.e. Behenic acid)
	n-hexadecanoic acid (i.e. Palmitic
	acid)
Other alkanes and derivatives	glycerol monostearate
methylcylohexane	
cyclohexane	**Waxes and oil**
1-bromododecane	cottonseed oil
	palm oil
Esters	rapeseed oil
Isopropyl acetate	sunflower seed oil
butyl acetate	petrolatum (i.e. Vaseline)
Isobutyl acetate	bees wax
	shellac orange
Ketones	
2-undecanone	**Other**
	PEG stearate